

Original Research

Pollution Distribution from Korlaće Mine Pit into the Environment

Milica Tomović^{1*}, Irma Dervišević¹, Dragan Manojlović^{2,3},
Jelena Đokić¹, Marija Janačković¹

¹University of Priština, Faculty of Technical Sciences, Knjaza Miloša 7, 38220 Kosovska Mitrovica, Serbia

²University of Belgrade, Department of Analytical Chemistry, Innovation Centre, Faculty of Chemistry, Studentski Trg 12-16, Belgrade 11000, Serbia

³South Ural State University, Lenin Prospect 76, 454080 Chelyabinsk, Russia

Received: 18 April 2022

Accepted: 4 October 2022

Abstract

This paper presents the use of a software application for protection of the environment through modelling and simulation of air and soil pollution at the industrial waste deposit of Korlaće, Serbia, asbestos mine pit. In cases of abandoned mines, with a proper surveillance not being possible, a modelling-based pollution assessment is of utmost importance in implementation of measures for reduction and mitigation of the impact of dangerous waste deposits. For that purpose, a simulation of various climatic conditions typical of this region has been conducted - humidity 20%, air speed 2-7 m/s, and temperature range of -10 to 36°C. Because of the minor probability for greater air speed in this area they have not been examined. The calculation has been done by means of SCREENVIEW software, and the obtained results have been compared with the investigation results of the samples taken from the site. The calculated results have shown a nice agreement with the experimental values, which demonstrates the applicability of the software application.

Keywords: asbestos, abandoned mine Korlaće, dust emission, environment, modelling and simulation

Introduction

Rapid urbanisation and industrialisation, along with globally fast developmental processes, have all contributed to environmental degradation [1]. In some regions, industrial development has led to a significant increase in air pollution [2]. During the XX century, the changes brought about created a process which was having a permanent influence on almost all earthly

organic creatures [3]. The intensive exploitation of mineral sites was a major reason for an increase in soil, air, and water pollutants [4-16]. Ever growing human population worldwide is due to an irrational use of the planet's limited resources. Some of the most important issues caused by humans include environmental pollution, narrower living space, global climate changes, and species' extinction due to the ever exceeding human desire to exploit resources [17]. The papers published by scientists predict that the number of world population living in cities should exceed the the range of 60-90% by 2030s [18]. Air pollution is considered one of the most important problems in the environment,

*e-mail: milica.tomovic@pr.ac.rs

and it impacts essential prerequisites for a healthy life in a negative fashion [19-21]. The air pollution represents a global issue, and worldwide estimates point to it being the cause of at least 1 to 8 death cases of humans. All the facets of air pollution impact human health significantly, and therefore air pollution investigations are really necessary for residential areas [19].

Asbestos (gr. ἄσβεστος -non-combustible) is the universal name for all asbestos minerals, and represents an integral part of the natural surroundings in the soil, rock masses and sediments [22], and it belongs to a group of silicate minerals with fibrous and crystal structure in the form of long, thin, and flexible fibers, resistant to traction and almost chemically inert [23-29]. Ever since the Stone age, humans have been using asbestos minerals [30] in small quantities and intermittently for thousands of years. In 1880, a modern industrial application began, with Quebec chrysotile fields being exploited, at the beginning of the XX century, there was a gradual increase and application of asbestos [31]. Asbestos mineral fiber is affordable and geographically ubiquitous [32]. In nature, it appears as polyfilamentous fiber bundles, and presents a unique morphology [33]. Because of its unique characteristics, as well as chemical and physical features, asbestos represents a wide spectrum for industrial raw materials, including construction industry, as well as products resistant to heat and abrasion [33, 34]. By the time the industrial usage of asbestos reached its peak, there had been more than 3000 different kinds of products [35, 36], even though most of these products are not produced today [37]. Asbestos is the term applied to certain fibrous minerals, and it appears in two forms naturally - serpentine and amphibole [23, 28-39]. Chrysotile belongs to the serpentine family, whereas other forms of asbestos belong to a subgroup of the amphibole family [40, 41]. Worldwide, chrysotile asbestos is the most widely used (90%-95%) [42]. Chrysotile, as the main form of commercial asbestos, better known as white asbestos, has been used as a raw material in the production of brake pads and clutch pads of automobiles since the 1900s [43, 44]. Based on its characteristics, such as high heat resistance and flexibility, chrysotile is most often used for the production of ceramics, thermal and acoustic insulation, films, papers, textiles, asbestos cement, adsorbents and catalysts [45-50].

Morphological composition of asbestos is shown in Table 1.

For more than a hundred years, asbestos has been widely used commercially [51, 52], while globally, some 125 million people are occupationally exposed to it every year [53]. Asbestos fibres are heat and fire-resistant [54], and it also has antiseptic and insulating properties [55], not disintegrating by means of biological methods, not dissolving in water, and not evaporating, asbestos fibres do not have a distinctive taste or odour, and show high strength and a good "flaking ability" [56-58]. Asbestos has been attracting ever greater attention due to possible health risks associated with it [22]. The investigations carried out in the past tell us of an important relationship between the air pollution and illnesses such as cardiovascular diseases, asthma or lung cancer [19] as well as an increase in early death rates [4, 8, 10, 20, 59, 60]. Asbestos is not harmful because of its chemical composition, but because of its needle-shaped structure, which could easily penetrate lung membranes, which presents a danger. One of the emerging risks is presence of its fibres in the air that humans can be exposed to [22, 61] as such, they can be inhaled into the lungs, stomach or body [62] and cause diseases that mainly affect the respiratory system [63]. Particles may be defined as liquid or hard substances floating in the air [64]. The hard substances are researched in such a great volume because one of the most important reasons for such practice is their being of tiny sizes. These tiny particles present a significant concern, and are investigated due to their ability to penetrate deeply into the lungs or to be inhaled and absorbed in the bloodstream, causing serious health problems [19]. The investigations show that exposition to those particles could lead to a significant increase in illness and death rates, particularly including those already contaminated with heavy metals [65-70]. Heavy metals, even in small concentrations, can have toxic and cancerous influence on humans, and remain in nature for a long time without being decomposed – they also bio-accumulate in living organisms, which may perish with their higher concentrations [2, 71]. Consequently, continual investigation of heavy metals' pollution is of utmost importance [72]. There are two ways in which the environment is polluted – natural and anthropogenic (human-caused), including pollutants emitted through

Table 1. The Regulated Asbestos Minerals [40].

Regulatory Name	Mineral Name	Mineral Group	Ideal Chemical Formula
Chrysotile	Chrysotile	Serpentine	$Mg_3Si_2O_5(OH)_4$
Tremolite	Tremolite	Amphibole	$Ca_2Mg_5Si_8O_{22}(OH)_2$
Actinolite	Actinolite	Amphibole	$Ca_2(Mg,Fe^{2+})_5Si_8O_{22}(OH)_2$
Anthophyllite	Anthophyllite	Amphibole	$Mg_2Mg_5Si_8O_{22}(OH)_2$
Crocidolite	Crocidolite	Amphibole	$Na_2(Fe^{2+}_3, Fe^{3+}_2)Si_8O_{22}(OH)_2$
Amosite	Cummingtonite- Grunerite	Amphibole	$Mg_2Mg_5Si_8O_{22}(OH)_2 - Fe_2Fe_3Si_8O_{22}(OH)_2$

industrial activities, which remain in nature for a long time and have a harmful influence on people's health [66]. Asbestos fibers, fine dust (particles) and heavy metals in regions with natural asbestos can be emitted into the atmosphere from natural and anthropogenic sources, naturally from rocks and soil containing asbestos and artificially through human activities that have a significant impact on the environment [73-81]. The use of chrysotile fibers is regulated, and in some countries its even banned (more than 50 countries) [82, 83], since asbestos is now known to be carcinogenic and it causes lung cancer, larynx and ovary cancer, asbestosis and pleural mesothelioma [84-88]. The air surrounding us impacts our everyday lives significantly, and the air we breathe should be clean in order to live a healthy and productive life, not to mention the importance of soil [89, 90]. The soil has quite a significant role in the functioning of the ecosystem [89]. The greatest risk of air pollution can be found at vast abandoned asbestos mines, whose asbestos waste causes serious environmental pollution [22, 91]. Considering the importance of environmental monitoring, especially in cases of an identified polluter, the aim of this paper is to assess a possible negative impact of the deposit and slag heap on people's health and the environment, and verify the relevance of the SCREENVIEW software programme, which is used for simulation modelling of the environmental pollution, by means of investigation and analysis of physical, chemical, and mineralogical composition of real samples taken from the sediments closest to the mine and slag heap. In order to calculate the range of pollution and the pollutants' concentration at close distances from the source, a specialised software package has been used. SCREEN3, version 3.0 of the SCREEN model has been developed to provide a method for obtaining pollutant concentration estimates by performing all short-term calculations for a single source, and, especially, for estimating maximum ground-level concentrations and the farthest distances, including the effects of flat and elevated terrains on maximum concentrations, and modelling the effects of simple volume sources using a virtual point source procedure.

In this case, the calculation has been done for AREA source, and includes the following initial data:

- emission rate - determined as emission rate per unit area, in this case ($\text{mg}/\text{m}^2/\text{s}$), in controlled laboratory conditions,
- source release height determined from the terrain cross-section,
- larger side length of rectangular area: 2510 m,
- smaller side length of rectangular area: 860 m,
- analysis of the range of wind directions: The maximum concentration of the pollutant should be observed in the direction downwind from the landfill.

For the purpose of modelling, the landfill is envisioned to be a rectangular area, and the downwind direction is calculated against the larger side length.

The research has been expanded on all stability classes and wind directions, so as to find the maximum impact. The site chosen for investigation is Korlaće asbestos mine in Serbia.

Near Brvenik in the Ibar valley, on the slopes of Korlaće stream and at the altitude of 600-800 m there is a deposit of chrysotile-asbestos [92, 93]. Asbestos ore was discovered in this area in 1939 [94]. Korlaće mine began working during WWII, and the regular production started after the war, in 1946 [95]. Korlaće stream divides the deposit into two parts - there are "Leštak" and "Stanilovica" on its right slope, in the NW-SE direction, and "Pogrebine" and "Bučje" on its left slope in the NE-SW direction [96]. The mineral subsoil with chrysotile-asbestos was formed in the crushed zone between serpentinite and dacite-andesite in the length of up to 1500 m [92]. The deposit comprises serpentinite groups and belongs to transverse-fibrous variety. Asbestos belongs to the reticulate type of minerals, and within the deposit it is found in rimmed veins [94]. The most characteristic physical feature of Korlaće serpentinites is their colour with all the shades of greenish-white to dark (almost black) green [96]. Their colourful appearance mostly depends on the presence of iron oxides and hydroxides [96]. The Fig. 1 shows a Korlaće serpentinite which displays all the colour shades characteristic for that kind of ore.

Based on the intensity and level of damage, three zones may be distinguished - the first zone includes better preserved serpentinites with larger blocks; the second one is a zone of crushed serpentinite; and the third one being a zone of superficially decomposed and ground serpentinite [96]. At the factory, where the ore was processed, it contained 1-2% of asbestos [97]. The ore was broken, crushed, and turned into the tiniest dust from which fibrous asbestos was extracted [97]. The ore's dust was to be found on all factory and mine premises, and it was a major harmful factor [97]. Asbestos exploitation was conducted in the vicinity of the mine, and slag heaps were places where the processed serpentinite residua, carrying



Fig. 1. Korlaće serpentinite.

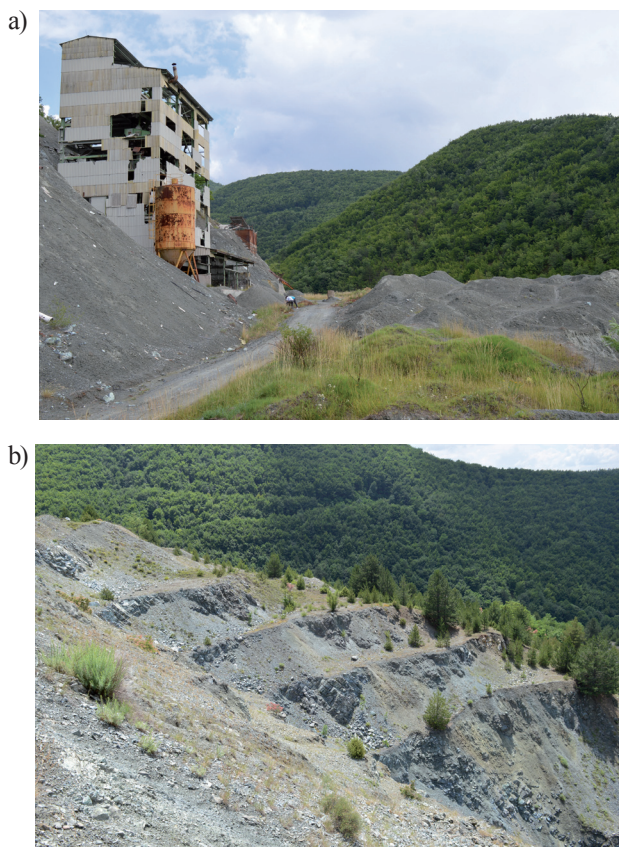


Fig. 2. Abandoned asbestos mine – Korlaće, a) former factory, b) a site section.

a certain percentage of asbestos residua, were disposed of. The Fig. 2a) shows the ore-processing factory, which represents one of the most harmful factors, due to the presence of the tiniest dust both inside the factory itself and in its immediate surroundings, and it is emitted into the atmosphere. The Fig. 2b) shows a part of the serpentinite deposit.

Material and Methods

For the purpose of this site's investigation and demonstration of the constancy of asbestos in the immediate surroundings of the asbestos mine itself, a sampling adapted to the terrain morphology has been carried out. In total, 30 different samples have been analysed.

Chemical analyses of the Korlaće site samples have been done by using SEM-EDS on JEOL JSM-6610LV. Quantitative chemical analysis has been done by using an EDS detector (model: X-Max Large Area Analytical Silicon Drift connected with INCAEnergy 350 Microanalysis System) with element detection possibilities of $Z \geq 5$ and detection limit of ~ 0.1 mas. %, with resolution of 126 eV. The analysing process has made use of standard natural minerals of aluminosilicates of the MAC company. As a source of electrons, a W filament has been used. Analyses have

been conducted in ultra high-vacuum conditions, with 20kV of electron acceleration voltage and 10mA of current power. The XRD analyses have been carried out for the purpose of detection of phases present in the examined samples, and they have been done by using a D2 PHASER device of the Bruker company. The device was equipped with a dynamic scintillating detector and a ceramic X-ray Cu tube (KFL-Cu-2K) in the range of 2θ from 5° to 75° .

The contents of major and trace elements were determined by inductively coupled plasma optical emission spectrometry (ICP-OES). ICP-OES measurement was performed using Thermo Scientific iCAP 6500 Duo ICP (Thermo Fisher Scientific, Cambridge, United Kingdom). For total dissolution of samples was performed on Advanced Microwave Digestion System (ETHOS 1, Milestone, Italy) using HPR-1000/10S high pressure segmented rotor. After the addition of the appropriate concentrated acids, the samples were then heated with microwave energy for 30 min. The temperature was gradually raised to 220°C in the first 10 min, remained at 220°C in the next 20 min, and then decreased rapidly to room temperature. All reagents were analytical grade reagents purchased from Sigma Aldrich, Germany. Four plasma standard solutions were used to prepare calibration solutions for ICP-OES measurement: Multi-Element Plasma Standard Solution 4, Specpure®, 1000 $\mu\text{g/ml}$ (purchased from Alfa Aesar GmbH & Co KG, Germany) and SS-Low Level Elements ICV Stock, ILM 05.2 ICS Stock 1 and Hg Calibration Stock (10 mg/L Hg) (purchased from VHG Labs, Inc-Part of LGC Standards, Manchester, NH 03103 USA).

The software used was an ArcGIS Desktop software, ArcMap 10.8.1 licensed software, of the ISRI company. It is used for creating maps, conducting geo-spatial analyses, and for management and presentation of geographical data.

Apparatus for the measuring of solid particles carried by the wind is composed of the fan type ABVE-3,5 with flow of $3600 \text{ m}^3/\text{h}$, vacuum of 200 Pa, used for air flow simulation, gravimetric sampler of the respiratory dust, the sample set in shallow metal plate, measuring scale for the residual solid particles on the filter paper and digital anemometer (DA-4000). The measurements are performed with material set in the air flow direction from the fan, and before the apparatus for polluted air vacuuming. The measurements were performed in wind velocity of 3 m/s, as average in the given area. The humidity in the laboratory was 20%.

Results and Discussion

For the purpose of the site's investigation and demonstration of the constancy of asbestos in the immediate surroundings of the asbestos mine itself, a sampling adapted to the terrain morphology has been

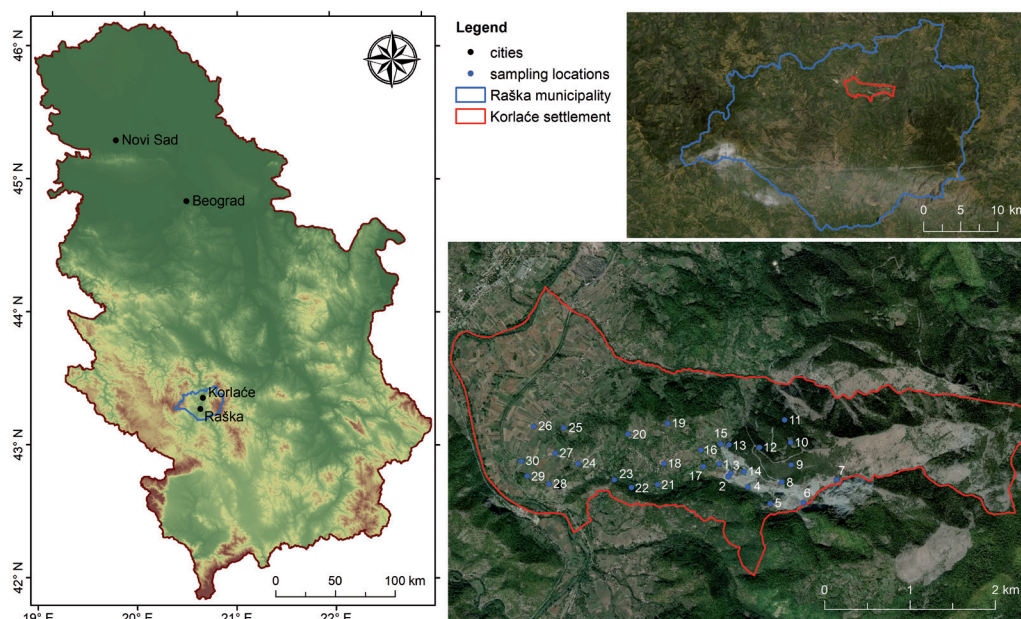


Fig. 3. Studied area map with sampling locations.

carried out. In total, 30 different samples collected at the site have been analysed. The investigated site Korlaće belongs to Raška district, situated between $43^{\circ}36'-43^{\circ}38'$ and $20^{\circ}63'-20^{\circ}71'$ in the southwestern part of Serbia (Fig. 3). According to the 2002 census, it had 529 inhabitants [98]. Korlaće is located 11 kilometres downstream from Raška, on the right bank of the Ibar River. As a community cadastre, it covers an area of 1022 ha. Along the extended Kopaonik massif, it is blocked by Pogrebina to the east, to the north it is separated from villages Piskanje and Kuriće by the Kuriće stream, to the south is the village of Zutice, and the Ibar to the west [99].

This region is characterised by temperate continental climate, with average annual temperature of about 14°C and precipitation being 32-97 mm (Republic Hydrometeorological Institute of Serbia). The site's altitude reaches 582 m, whereas sampling altitudes were between 500 and 810 m. The sampling locations were selected by using the hypothesis of a progressive subsidence of the chosen elements' contents with an increase in distance against the industrial facility.

The sampling methodology itself has been conducted in accordance with the IUPAC recommendations on soil sampling [100]. The grounds have been sampled with a stainless-steel probe at the depth of the soil (0-20 cm), where the largest mass of roots has been found. Upon obtaining a composite sample, leaves, non-dissolvable residua, rocks, roots, and other visible impurities have been removed. The dust in the facility's immediate surroundings has been sampled in accordance with regulations [101] by wearing adequate equipment necessary for proper sampling of asbestos. Each sample weighs 0,5 g for the purpose of SEM-EDS analyses, whereas the XRD analysis required the sample's mass to weigh 1 g.

In order to examine the distribution of asbestos fibres and heavy metals as per grain shapes and sizes, the samples collected at the investigated site have undergone a scanning electron microscopy. All the samples, shown in Table 2, having been thoroughly examined, the search for eventual heavy metals has continued by dot scanning. Chemical composition and form of the compound have been determined with more accuracy. The first examined sample (sample 1, Table 2) is a combination of samples taken at the facility itself and in its immediate surroundings. The sample is dim greenish with white colour impurities, and it has been determined to compose of microscopically thin flossy fibres whose size measures $4-50\ \mu\text{m}$ of the plate and column parts. SEM-EDS analysis reveals that the sample is mostly made up of quartz, talc, magnesite, magnetite, and of serpentinite. The samples do not present bright particles with contents of heavy metals, which has been corroborated by the composition shown in Table 2. In the sample 1's microphotography, magnified by 2000 times (see Fig. 4a), one can observe a fibrous texture of fibriform minerals overlapping one another. The manner of appearance of the mineral, its crystal form and chemical composition, all indicate that the examined mineral belongs to the serpentinite group. The arrow points to fibrous filament of asbestos. Based on the sampling location of the collected sample, it is quite clear that the sample contains chrysotile, so-called white asbestos, the morphology of which is made up of thin and flexible fibres. The Fig. 4b) demonstrates a proportionally large column-like part of antigorite, whereas the Fig. 4c) shows the plate-like part of lizardite. This confirms the fact that in the past the Korlaće mine exploited asbestos as a raw material for manufacture of thermal insulators, bricks for high-temperature furnaces, or pipes for construction industry.

Table 2. EDS analysis of the surface of the sample Korlaće.

Sample	O wt.%	Mg wt.%	Al wt.%	Si wt.%	Ca wt.%	Fe wt.%	Cu wt.%	Na wt.%	K wt.%	Total
1.	56.50	21.63	0.55	17.04	0.48	3.45	0.35	0.00	0.00	100.00
2.	56.04	22.38	0.49	16.34	0.25	3.55	0.95	0.00	0.00	100.00
3.	56.82	21.71	0.50	17.28	0.38	2.62	0.69	0.00	0.00	100.00
4.	47.44	19.83	1.19	29.08	0.29	2.17	0.00	0.00	0.00	100.00
5.	53.88	24.23	0.52	19.80	0.00	1.57	0.00	0.00	0.00	100.00
6.	54.32	21.33	0.73	19.75	0.00	3.31	0.56	0.00	0.00	100.00
7.	51.74	16.90	2.89	20.32	0.69	6.53	0.93	0.00	0.00	100.00
8.	55.01	23.13	0.39	19.41	0.00	2.06	0.00	0.00	0.00	100.00
9.	55.75	8.13	4.89	21.58	1.99	5.94	0.00	1.72	0.00	100.00
10.	55.69	8.54	5.36	20.41	1.73	6.81	0.00	1.46	0.00	100.00
11.	57.44	19.97	0.52	15.75	3.39	2.93	0.00	0.00	0.00	100.00
12.	51.07	4.48	4.89	19.25	1.11	6.02	0.00	1.18	0.00	100.00
13.	52.36	21.05	0.87	21.24	0.67	2.98	0.83	0.00	0.00	100.00
14.	54.58	19.94	1.79	19.14	0.54	4.01	0.00	0.00	0.00	100.00
15.	52.91	19.86	1.41	19.67	0.67	4.51	0.97	0.00	0.00	100.00
16.	53.52	5.78	6.48	23.80	1.26	7.68	0.00	1.48	0.00	100.00
17.	54.79	17.89	1.90	17.58	2.54	5.30	0.00	0.00	0.00	100.00
18.	53.71	4.49	6.77	23.68	1.27	6.38	0.82	1.18	1.70	100.00
19.	52.72	5.66	5.93	24.55	1.02	7.45	0.32	1.39	0.96	100.00
20.	53.08	5.50	5.99	23.71	1.06	7.73	0.75	1.16	1.02	100.00
21.	54.36	5.47	6.08	22.79	0.95	7.36	0.46	1.32	1.21	100.00
22.	53.78	4.98	6.71	22.38	1.04	7.71	0.85	1.32	1.23	100.00
23.	54.12	4.76	5.78	23.51	1.48	7.37	0.64	1.19	1.15	100.00
24.	53.55	5.30	6.25	22.10	1.04	8.63	0.91	0.77	1.45	100.00
25.	51.09	5.15	6.68	24.07	1.06	8.03	0.87	1.57	1.48	100.00
26.	52.96	4.62	6.10	23.96	1.68	7.89	0.35	1.37	1.07	100.00
27.	54.08	4.18	6.38	23.15	1.37	7.56	0.52	1.35	1.41	100.00
28.	52.98	21.03	0.96	16.98	2.85	4.02	0.00	1.18	0.00	100.00
29.	53.97	5.87	6.26	22.08	1.58	6.36	0.87	1.54	1.47	100.00
30	53.54	2.63	7.89	25.34	1.23	6.67	0.00	1.03	1.67	100.00
Mean	53.79	12.55	3.77	21.19	1.12	5.49	0.42	0.74	0.53	100.00
St. Dev.	1.96	8.00	2.69	3.09	0.81	2.16	0.39	0.68	0.67	100.00
Minimum	47.44	2.63	0.39	15.75	0.00	1.57	0.00	0.00	0.00	100.00
Maximum	57.44	24.23	7.89	29.08	3.39	8.63	0.97	1.72	1.70	100.00

Fig. 5 shows an XRD diffractogram of the sample 1. On the basis of the EDS chemical analysis and XRD diffractogram, it can be concluded that the investigated sample from Korlaće site belongs to the serpentinite group. Based on their morphology and

XRD analysis, three types of serpentinite have been determined:

- antigorite, with proportionally the largest presence in the sample, and naturally it is green, greenish-blue, brown or black in colour,

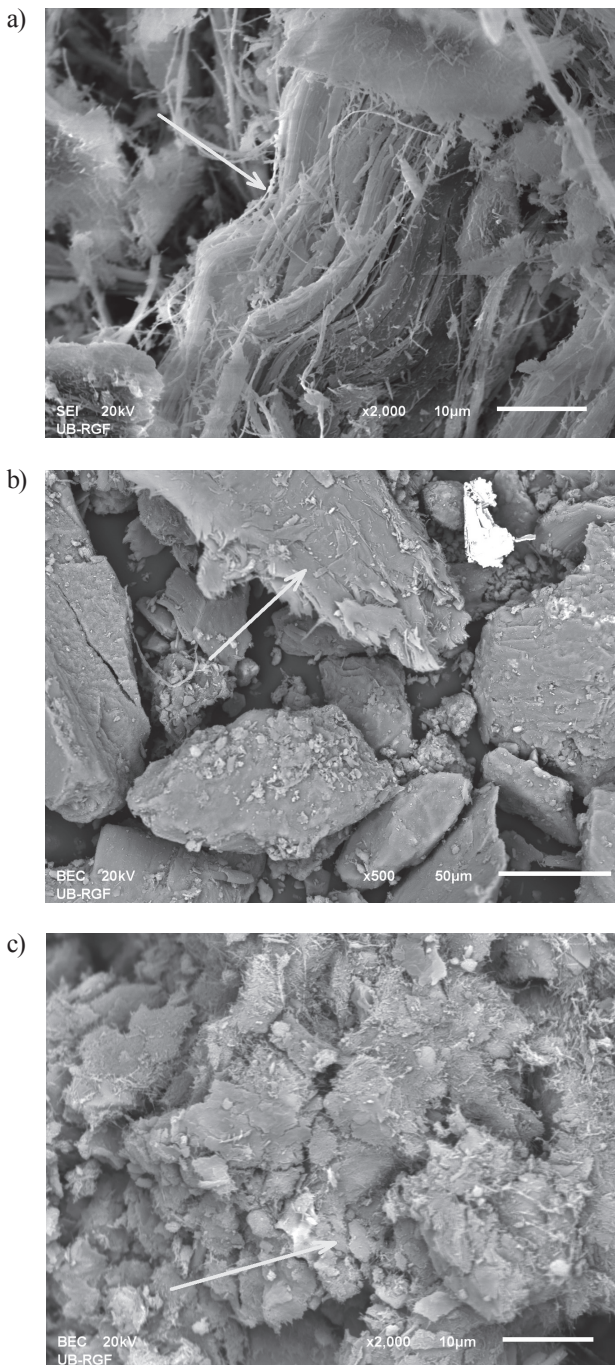


Fig. 4. SEM-EDS analysis of the sample 1: a) SEM image of the chrysotile, b) SEM image of the antigorite and c) SEM image of the lizardite.

- chrysotile, the sample's second component after antigorite, presents one of the biggest problems due to its needle-shaped structure, and
- lizardite, light-yellow to greenish-brown in colour.

Besides serpentinite $\text{Mg}_3\text{Si}_2\text{O}_5(\text{OH})_4$ the sample contained talc $\text{Mg}_3(\text{OH})_2\text{Si}_4\text{O}_{10}$, quartz SiO_2 , magnetite Fe_3O_4 and fosterite $(\text{Mg}_{0.6}\text{Fe}_{0.4})_2\text{SiO}_4$.

The second examined sample (sample 16, Table 2) is mostly brown in colour, with a small quantity of microscopically detected plant residua mixed with some fine-grained matter. The grain size is about 2-10 μm ,

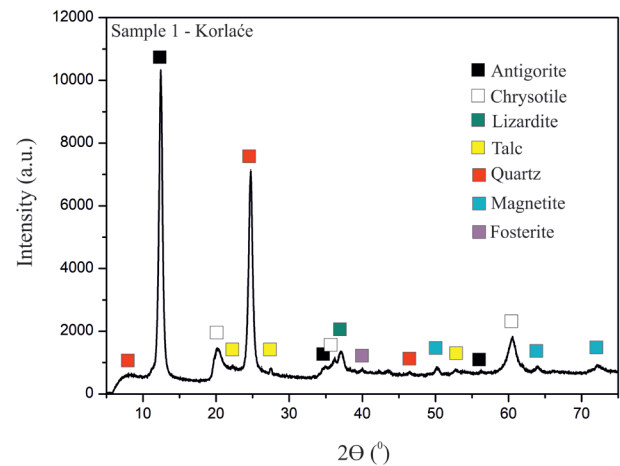


Fig. 5. XRD diagram of the sample 1.

with occasional agglomerates as big as 100 μm . The agglomerates are rounded, while some more magnified individual grains present agglomerates with irregular edges. The Fig. 6 shows the SEM microphotography of the sample 16.

The map (Fig. 3) displays the location for the sample 16 in the immediate surroundings of the abandoned mine - it is an arable area. SEM-EDS analysis reveals the sample to be made up mainly of a mixture of quartz, clay minerals, iron oxides, and aluminium. In Fig. 6b), with a 200x magnification and dot scanning, the presence of antigorite has been determined, and confirmed by the XRD analysis. On the basis of the chemical composition given in Table 2, (sample 16) and the XRD analysis, the presence of the following chemical compounds has been determined: quartz SiO_2 , antigorite $\text{Mg}_3\text{Si}_2\text{O}_5(\text{OH})_4$, hematite Fe_2O_3 , talc $\text{Mg}_3(\text{OH})_2\text{Si}_4\text{O}_{10}$, malliss clay Ca-Mg-Al-Si-O , magnesium silicate $\text{Mg}_2(\text{Si}_2\text{O}_6)$, corundum Al_2O_3 and kaolinite $\text{Al}_2(\text{Si}_2\text{O}_5)(\text{OH})_4$ (Fig. 7).

The third examined sample (sample 30, Table 2) is brownish in colour, with differently sized agglomerates (5-10 μm), and some larger ones may be observed (Fig. 8). This sample contains some vegetal residua. SEM-EDS analysis reveals the sample 30 to be made up of quartz and clay minerals.

On the basis of the SEM-EDS chemical analysis, the following results have been obtained: the sample contains quartz SiO_2 , talc $\text{Mg}_3(\text{OH})_2\text{Si}_4\text{O}_{10}$ and clay $\text{CaMg}_2\text{AlSi}_4(\text{OH})_2\cdot\text{H}_2\text{O}$ (Fig. 9).

Besides the SEM-EDS chemical analysis and the XRD compound detection, some samples have been analysed by means of ICP-OES in order to detect trace elements. For the purpose of examination of the sample's chemical composition on ICP-OES, the ground samples have been homogenised and dried at 105°C, in an agate mortar. The first sample is a crushed serpentinite collected from the factory building location (sample 1, Table 2), and the second examined sample is a separated chrysotile, so-called white asbestos (sample 8, Table 2). The Table 3 shows detected concentrations of

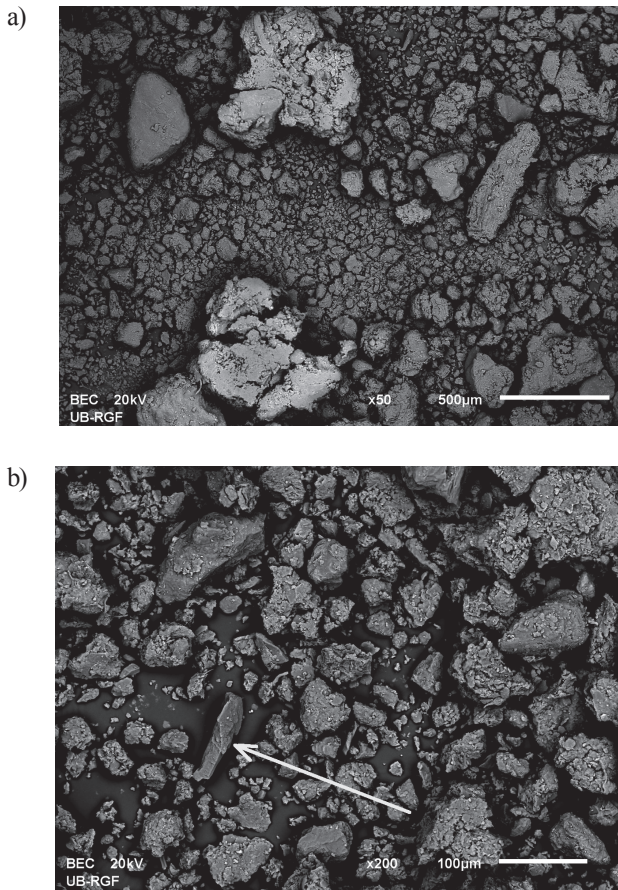


Fig. 6. SEM-EDS analysis of the sample 16: a) SEM image of the soil, and in b) antigorite pointed to with a arrow.

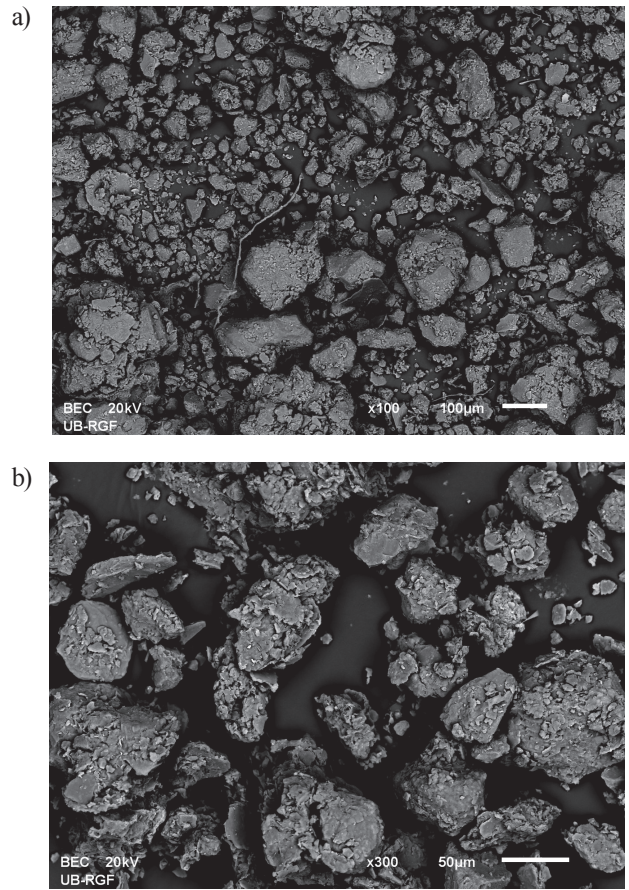


Fig. 8. SEM-EDS analysis of the sample 30 (a, b - SEM image of the soil with magnification of x100 and x300).

elements (in ppm) in the samples of serpentinite and asbestos.

Besides the main elements that form the composition of serpentinite and chrysotile, such as Mg, Ca, Al in traces, 20 additional chemical elements have been discovered - B, Ba, Cd, Co, Cr, Cu, Fe, Hg, K, Li, Mn, Mo, Na, Ni, Pb, S, Sb, Se, Sr, and Zn, many of which are

extremely dangerous for the environment and people's health. Inhalation of airborne fibres presents a risk for human health. Depending on the size, particularly dangerous are dust particles in the size range of 2,5 µm and less, which may penetrate pulmonary alveoli. Once introduced into the organism/lungs, never again can they be eliminated [102].

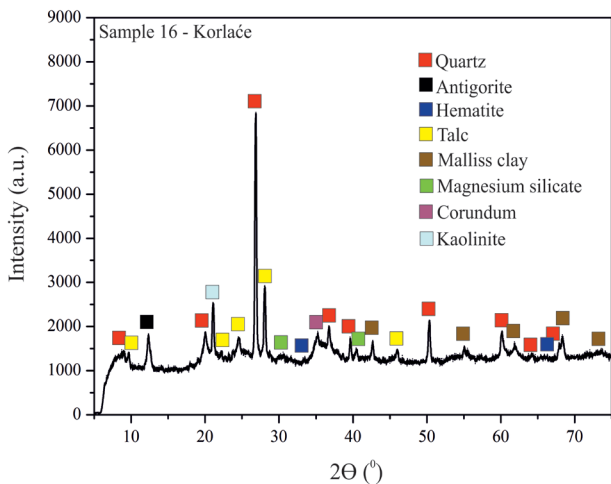


Fig. 7. XRD diagram of the sample 16.

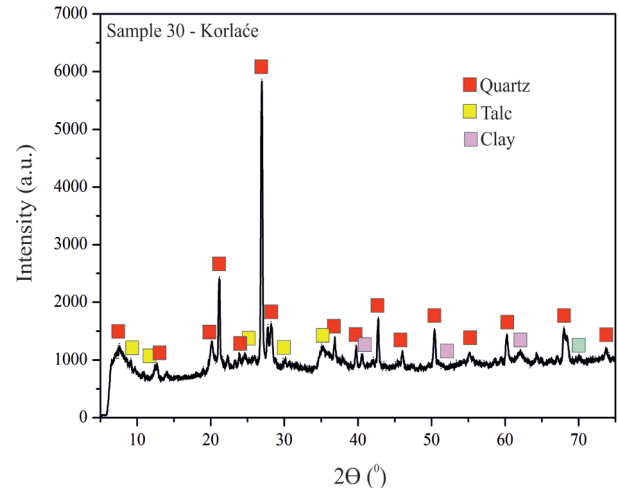


Fig. 9. XRD diagram of the sample 30.

Table 3. Composition determination of trace elements (ppm) by using ICP-OES.

Elements	Sample 1 - Korlaće (ppm)	Sample 8 – Korlaće (ppm)
Al	4642.01	6219.63
B	39.65	33.71
Ba	3.36	0.32
Ca	11189.02	171.19
Cd	0.33	0.11
Co	52.64	29.72
Cr	929.29	10.65
Cu	11.08	/
Fe	31404.31	15170.07
Hg	0.02	0.01
K	141.32	24.67
Li	1.80	0.26
Mg	1745.51	1682.22
Mn	519.95	188.14
Mo	0.36	0.26
Na	2.94	10.18
Ni	1083.84	821.19
Pb	21.21	8.57
S	562.91	102.33
Sb	21.55	0.57
Se	0.27	0.01
Sr	5.43	/
Zn	33.67	19.48

Experimental evidence of an epidemiological study present indications for a possible occurrence of lung cancer due to the impact of heavy metals [101-104]. Ni, Cr, Zn, Pd, and Cd are mostly carcinogenic

and are industry-based [66]. Due to their impact and a potential toxicity, Hg, Pb, and Cd belong with the most poisonous heavy metals [105, 106] even in small concentrations [107]. Mn, Cr, Cu, Fe, Ni, and Zn may also have a detrimental impact in high concentrations [106]. On the basis of the obtained results, a special attention is dedicated to heavy metals, such as Cr, Ni, Co, Zn, Pb, and Hg, according to their impact on human health [108, 109]. One of the elements that represents serious consequences for human health is Pb, if the body absorbs the impact on the digestive and respiratory system [110]. Previous medical research has not linked the development of lung cancer due to Co exposure but it has been shown that Co is absorbed into the bloodstream or muscle tissue and can cause several cardiovascular, endocrine and neurological deficits [111]. Asbestos fibers and trace elements Mn, Co, Ni, Co reach the environment due to natural or anthropogenic activities, which leads to environmental contamination and endangering human health [112-115]. It may be concluded that the examined samples contained increased concentrations of Ni and Cr [112, 116, 117], which can have a negative impact on the human health and the environment [118, 119].

The laboratory tests for dust loading were performed for the asbestos bearing mining waste. The results obtained for climate conditions of stable weather when the actual measurements are performed are included as initial data in SCREENVIEW software, and the diagram showed reasonable agreement with measured values from the Fig. 10, in given climate conditions (wind speed 3 m/s, relative humidity 20%). Based on that assumption, the laboratory data are included for the untreated and solidified asbestos bearing waste for all stability classes for the full meteorology and the results are shown in Fig. 10. It is clearly observed that MAC for airborne dust loading for untreated asbestos waste deposit is reached after 450 m for the average wind speed of 3 m/s.

Taking into consideration all the wind classes, the results of airborne dusting ($\text{mg}/\text{m}^2/\text{s}$) in the laboratory, as initial data, for a relative humidity of 20 %, are presented in Fig. 11.

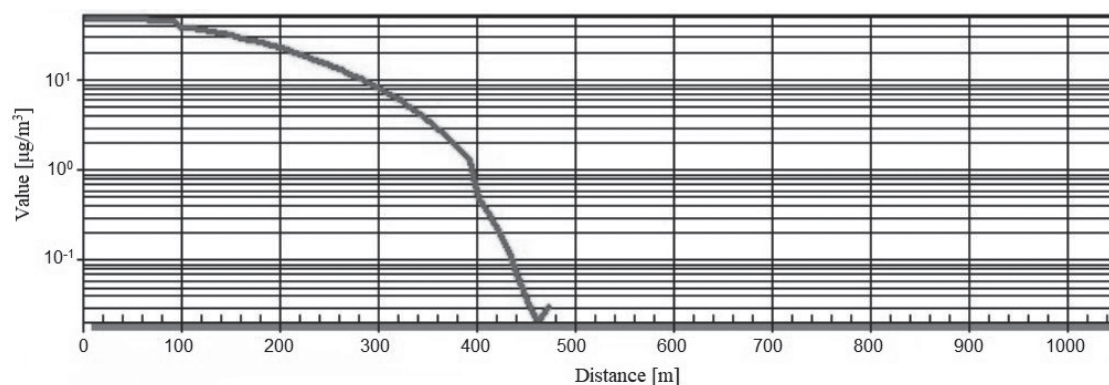


Fig. 10. Calculated concentration of Asbestos bearing particles for the relative humidity of 20% in the full meteorology conditions.

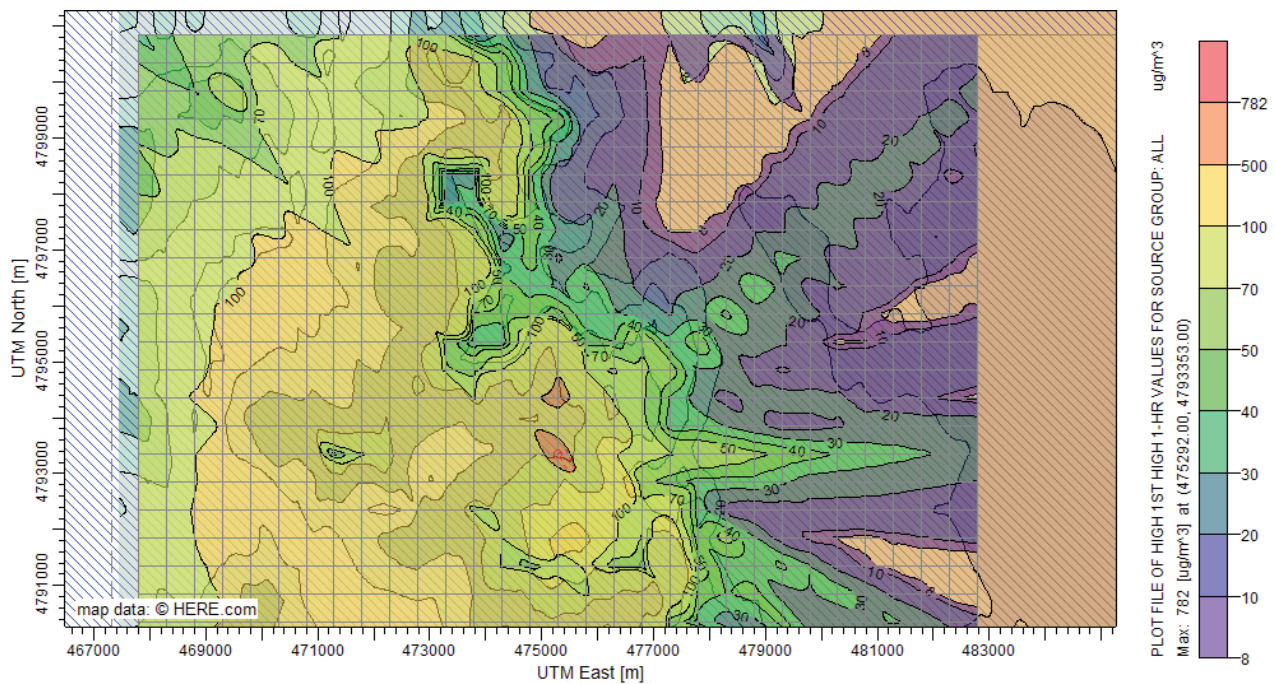


Fig. 11. Asbestos bearing particles scattering range from the mining waste Korlaće for all stability classes.

Conclusions

Asbestos bearing mining waste Korlaće is proven to be environmental hazard due to the small grained particles containing asbestos. The simulation made by using software application can be useful in environmental impact assessment as the abandoned deposit is situated in a remote mountain area, and the regular monitoring was not set on site. According to the simulation, the asbestos bearing particles concentration has exceeded the MAC of 0.1 g/m^3 for the distance of 450 m for the single relatively stable wind class of 3 m/s, and for the distance of 2500 m for the full meteorology conditions, i.e. all stability classes. By analyzing the results of the calculation, it can be seen that the calculated values show the maximum ground-level concentration of the pollutant in the same area, and shows a reasonable agreement with the measured values on the ground. That suggests that using the SCREEN application is of help in initial analyses and facilitates ascertainment of land use and land management in an affected area.

Conflict of Interest

The authors declare no conflict of interest.

References

- SEVIK H., CETIN M., OZEL H.B., ERBEK A., ZEREN CETIN I. The effect of climate on leaf micromorphological characteristics in some broad-leaved species. *Environment, Development and Sustainability*, **23** (4), 6395, 2021.
- CETIN M., JAWED A.A. Variation of Ba concentrations in some plants grown in Pakistan depending on traffic density. *Biomass Conversion and Biorefinery*, 1-7, 2022.
- VAROL T., CETIN M., OZEL H.B. SEVIK H., CETIN I.Z. The Effects of Climate Change Scenarios on *Carpinus betulus* and *Carpinus orientalis* in Europe. *Water Air and Soil Pollution*, **233**, 45, 2022.
- ADIGUZEL F., CETIN M., KAYA E., SIMSEK M., GUNGOR S., SERT E.B. Defining suitable areas for bioclimatic comfort for landscape planning and landscape management in Hatay Turkey. *Theoretical and Applied Climatology*, **139** (3), 1493, 2020.
- ADIGUZEL F., BOZDOGAN S.E., DINC Y., CETIN M., GUNGOR S., YUKA P., DOGAN O.S., KAYA E., KARAKAYA K., VURAL E. Determining the relationships between climatic elements and thermal comfort and tourism activities using the tourism climate index for urban planning: a case study of Izmir Province. *Theoretical and Applied Climatology*, **147** (14), 1, 2021.
- BAYRAKTOR O.Y. Possibilities of disposing silica fume and waste glass powder, which are environmental wastes, by using as a substitute for Portland cement. *Environmental science and pollution research international*, **28** (13), 16843, 2021.
- BOZDOGAN SERT E., KAYA E., ADIGUZEL F., CETIN M., GUNGOR S., ZEREN CETIN I., DINC Y. Effect of the surface temperature of surface materials on thermal comfort: A case study of Iskenderun (Hatay, Turkey). *Theoretical and Applied Climatology*, **144** (1), 103, 2021.
- CETIN M. The effect of urban planning on urban formations determining bioclimatic comfort area's effect using satellite images on air quality: A case study of Bursa city. *Air Quality, Atmosphere & Health*, **12** (10), 1237, 2019.
- CETIN M. The changing of important factors in the landscape planning occur due to global climate change in temperature, rain and climate types: A case study of

- Mersin City. Turkish Journal of Agriculture-Food Science and Technology, **8** (12), 2695, **2020**.
10. CETIN M. Climate comfort depending on different altitudes and land use in the urban areas in Kahramanmaraş City. Air Quality, Atmosphere & Health, **13** (8), 991, **2020**.
 11. GUNGOR S., CETIN M., ADIGUZEL F. Calculation of comfortable thermal conditions for Mersin urban city planning in Turkey. Air Quality, Atmosphere and Health, **14** (4), 515, **2021**.
 12. SEVIK H., OZEL H. B., CETIN M., ÖZEL H. U., ERDEM T. Determination of changes in heavy metal accumulation depending on plant species, plant organism, and traffic density in some landscape plants. Air Quality, Atmosphere & Health, **12** (2), 189, **2019**.
 13. TURKYILMAZ A., CETIN M., SEVIK H., ISINKARALAR K., SALEH E.A.A. Variation of heavy metal accumulation in certain landscaping plants due to traffic density. Environment, Development and Sustainability, **22** (3), 2385, **2020**.
 14. UCUN OZEL H., GEMICI B. T., GEMICI E., OZEL H. B., CETIN M., SEVIK H. Application of artificial neural networks to predict the heavy metal contamination in the Bartın River. Environmental Science and Pollution Research, 1-18, **2020**.
 15. ZEREN CETIN I., SEVIK H. Investigation of the relationship between bioclimatic comfort and land use by using GIS and RS techniques in Trabzon. Environmental Monitoring and Assessment, **192** (2), 71, **2020**.
 16. ZEREN CETIN I., OZEL H. B., VAROL T. Integrating of settlement area in urban and forest area of Bartın with climatic condition decision for managements. Air Quality, Atmosphere & Health, **13** (8), 1013, **2020**.
 17. OZEL H.B., ABO AISHAL A.E.S., CETIN M., SEVIK H., ZEREN CETIN I. The effects of increased exposure time to UV-B radiation on germination and seedling development of Anatolian black pine seeds. Environmental Monitoring and Assessment, **193** (7), 388, **2021**.
 18. CETIN M., SEVIK H. Measuring the Impact of Selected Plants on Indoor CO₂ Concentrations. Polish Journal of Environmental Studies, **25** (3), 973, **2016**.
 19. ELSUNOUSI A.A.M., SEVIK H., CETIN M., OZEL H.B., OZEL, H.U. Periodical and regional change of particulate matter and CO₂ concentration in Misurata. Environmental Monitoring and Assessment, **193** (11), 707, **2021**.
 20. CETIN M., ONAC A.K., SEVIK H., SEN B. Temporal and regional change of some air pollution parameters in Bursa. Air Quality, Atmosphere & Health, **12** (2), 311, **2019**.
 21. CETIN M., SEVIK H. Change of air quality in Kastamonu city in terms of particulate matter and CO₂ amount. Oxidation Communications, **39** (4), 3394, **2016**.
 22. HARGITAI A., TOTTH E., VAŠKOVIĆ N., MILOŠEVIĆ M., WEISZBURG T.G. Abandoned chrysotile asbestos mines in Serbia: An environmental mineralogical study. Acta Mineralogica-Petrographica, Abstract Series, Szeged, **7**, 53, **2012**.
 23. GOLUBOVIĆ T., MILTOJEVIĆ A., GOLUBOVIĆ S., ILIĆ S. Asbestos-related occupational risks. IETI Transactions on Ergonomics and Safety, **2** (2), 22, **2018**.
 24. KUSIOROWSKI R., ZAREMBA T., PIOTROWSKI J., PODWORNÝ J. Utilisation of cement-asbestos wastes by thermal treatment and the potential possibility use of obtained product for the clinker bricks manufacture, Journal of Materials Science, **50** (20), 6757, **2015**.
 25. KOPYLEY L., CHRISTENSEN K.Y., BROWN J.S., COOPER G.S. A systematic review of the association between pleural plaques and changes in lung function. Occupational and Environmental Medicine, **72** (8), 606, **2015**.
 26. MILITELLO G.M., BLOISE A., GAGGERO L., LANZAFAME G., PUNTURO R. Multi-Analytical Approach for Asbestos Minerals and Their Non-Asbestiform Analogues: Inferences from Host Rock Textural Constraints. Fibers, **7** (5), 42, **2019**.
 27. LI J., DONG Q., YU K., LIU L. Asbestos and asbestos waste management in the Asian-Pacific 13 region: trends, challenges and solutions. Journal of Cleaner Production, **81**, 218, **2014**.
 28. CAVALLO A. Environmental asbestos contamination in an abandoned chrysotile mining site: the example of Val Malenco (central Alps, northern Italy). Journal of International Geoscience, **43**, 851, **2020**.
 29. MOTEALLEMI A., MINAEI M., TAHMASBIZADEH M., FADAEI S., MASROOR K., FANAEI F. Monitoring of airborne asbestos fibers in an urban ambient air of Mashhad City, Iran: levels, spatial distribution and seasonal variations. Journal of Environmental Health Science and Engineering, **18**, 1239, **2020**.
 30. TOTTH E., WEISZBURG T.G. Asbestos: A review with special emphasis on natural carpathian-dinaric occurrences. Acta Mineralogica-Petrographica, Abstract Series, Szeged **7**, 139, **2012**.
 31. SOEBERG M.J., LEIGH J., VAN ZANDWIJK N. Malignant mesothelioma in Australia 2015: Current incidence and asbestos exposure trends. Journal of Toxicology and Environmental Health, Part B, **19** (5-6), 173, **2016**.
 32. CUI Y., MA J., YE W., HAN Z., DONG F., DENG J., ZHANG Q. Chrysotile and rock wool fibers induce chromosome aberrations and DNA damage in V79 lung fibroblast cells. Environmental Science and Pollution Research, **25** (23), 22328, **2018**.
 33. DORLING M., ZUSSMAN J. Characteristics of asbestiform and non-asbestiform calcic amphiboles. Lithos, **20**, 469, **1986**.
 34. GHORBANI S., HAJIZADEH Y. Monitoring of airborne asbestos fiber concentrations in high traffic areas of Isfahan, Iran in summer 2015. International Journal of Environmental Health Engineering, **5**, 1, **2016**.
 35. REID G., KLEBE S., VAN ZANDWIJK N., GEORGE A.M. Asbestos and Zeolites: from A to Z via a Common Ion. Chemical Research in Toxicology, **34** (4), 936, **2021**.
 36. ROSNER D., MARKOWITZ G. "Ain't Necessarily Sol": The Brake Industry's Impact on Asbestos Regulation in the 1970s. American Journal of Public Health, **107** (9), e1-e5, **2017**.
 37. HENDERSON D.W., LEIGH J. The history of asbestos utilization and recognition of asbestos-induced disease. In: Dodson RF, Hammar S, editors. Asbestos: risk assessment, epidemiology and health effects. 2nd edition Boca Raton: CRC Press, 1-27, **2017**.
 38. MOKHTARI M., JAFARI N., EBRAHIMI A.A., MOHAMMADI A., ABDOLAHNEJAD A., HAJIZADEH Y., NIKNAZER H. Assessment of airborne asbestos fibers concentration in Yazd city in summer 2015. Journal of Environmental Health and Sustainable Development, **1** (2), 75, **2016**.
 39. BAEK S.C., KIM Y.C., CHOI J.H., HONG, W.H. Determination of the essential activity elements of an asbestos management system in the event of a disaster and their prioritization. Journal of Cleaner Production, **137**, 414, **2016**.

40. JOHN P.C., RONALD K.C., KJYOUNG L. Guidelines for Geologic Investigations of Naturally Occurring Asbestos in California. Special publication; California Geological Survey Public Information Offices: Los Angeles, CA, USA, **124**, 1, **2002**.
41. MOKHTARI M., JAFARI N., EBRAHIMI A., MOHAMMADI A., ABDOLAHNEJAD., HAJIZADEH Y., NIKNAZAR H. Assessment of airborne asbestos fibers concentration in Yazd city in summer 2015. *Journal of Environmental Health and Sustainable Development*, **1** (2), 75, **2016**.
42. ARTHUR F.L., JOSHU T.K. The global spread of asbestos. *Annals of Global Health*, **80** (4), 257, **2014**.
43. FATHABADI M.K.F., ABDOLAHNEJAD A., TEIRI H., HAJIZADEH Y. Spatio-seasonal variation of airborne asbestos concentration in urban areas of Shiraz, Iran. *International Journal Occupational and Environmental Health*, **23** (2), 143, **2017**.
44. BERNSTEIN D.M., ROGERS R.A., SEPULVEDA R., KUNZENDORF P., BELLMANN B., ERNST H., CREUTZENBER O., PHILIPS J.I. Evaluation of the fate and pathological response in the lung and pleura of brake dust alone and in combination with added chrysotile compared to crocidolite asbestos following short-term inhalation exposure. *Toxicology and Applied Pharmacology*, **283** (1), 20, **2015**.
45. ZAREMBA T., KRZAKALA A., PIOTROWSKI J., GARCZORZ D. Study on the thermal decomposition of chrysotile asbestos. *Journal of Thermal Analysis and Calorimetry*, **101**, 479, **2010**.
46. LIU K., ZHU B., FENQ Q., DUAN T. Novel transparent and flexible nanocomposite film prepared from chrysotile nanofibers. *Materials Chemistry and Physics*, **142**, 412, **2013**.
47. WANG X., LIN S., YANO E., YU I.T.S., COURTICE M., LAN Y., CHRISTIANI D.C. Exposure-specific lung cancer risks in Chinese chrysotile textile workers and mining workers. *Lung Cancer*, **85**, 119, **2014**.
48. PETKOWICZ D.I., RIGO R.T., RADTKE C., PERGHER S.B., DOS SANTOS J.H.Z. Zeolite Na/A from Brazilian chrysotile and rice husk. *Microporous Mesoporous Materials*, **116**, 548, **2008**.
49. SALINAS E.L., ANTONIO J.A.T., MANRIQUEZ M.E., CANTU M.S., RAMOS, I.C., CORTEZ J.G.H. Synthesis and catalytic activity of chrysotile-type magnesium silicate nanotubes using various silicate sources. *Microporous Mesoporous Materials*, **274**, 175-182, **2019**.
50. JIANG D.B., YUAN S., CAI X., XIANG G., ZHANG Y.X., PEHKONEN S., LIU X.Y. Magnetic nickel chrysotile nanotubes tethered with pH-sensitive poly (methacrylic acid) brushes for Cu (II) adsorption. *Journal of Molecular Liquids*, **276**, 611, **2019**.
51. ARTHUR F.L. Global use of asbestos - legitimate and illegitimate issues. *Journal of Occupational Medicine and Toxicology*, **15** (1), 16, **2020**.
52. MUSK A.W., DE KLERK N., REID A., HUI J., FRANKLIN P., BRIMS F. Asbestos-related diseases. *The International Journal of Tuberculosis and Lung Disease*, **24** (6), 562, **2020**.
53. HUGHES P.M.B.E., HUGHES P., FERRETT E. *International health and safety at work 3rd edition*, 400-401, **2015**.
54. KIM Y.C., HONG W.H., ZHANG Y.L. Development of a model to calculate asbestos fiber from damaged asbestos slates depending on the degree of damage. *Journal of Cleaner Production*, **86**, 88, **2015**.
55. BOURGAULT M., GAGNE M., VALCKE M. Lung cancer and mesothelioma risk assessment for a 16 population environmentally exposed to asbestos. *International Journal of Hygiene and Environmental Health*, **2**, 340, **2014**.
56. KAKOOEI H., NORMOHAMMADI M. Asbestos exposure among construction workers during demolition of old houses in Tehran, Iran. *Industrial Health*, **52**, 71, **2014**.
57. MARIORYAD H., KAKOOEI H., SHAHTAHERI S.J., YUNESIAN M., AZAM K. Assessment of airborne asbestos exposure at an asbestos cement sheet and pipe factory in Iran. *Regulatory Toxicology and Pharmacology*, **60**, 200, **2011**.
58. BURKHANOVA R.A., KOVTUNOV I.A., AZAROV V.N. Investigation of the Parameters of Discarded Dust in the Manufacture of Products from Chrysotile Asbestos and Cement. *IOP Conference Series: Earth and Environmental Science*, **272**, 022150, **2019**.
59. GRZEDZICKA E. Is the existing urban greenery enough to cope with current concentrations of PM_{2.5}, PM₁₀ and CO₂. *Atmospheric Pollution Research*, **10** (1), 219, **2019**.
60. HVIDTFELDT U., SEVERI G., SAMOLI E., ANDERSEN Z., HERTEL O., BRUNRKREEF B., BRUNEKREEF B., BOUTRON M., RAASCHOU-NIELSON O., FECHT D. Low-level ambient air pollution exposure and risk of lung cancer—a pooled analysis of 7 European cohorts. *Environmental Epidemiology*, **3**, 171, **2019**.
61. ZHA L., KITAMURA Y., KITAMURA T., LIU R, SHIMA M., KURUMATANI N., NAKAYA T., GOJI J., SOBUE T. Population-based cohort study on health effects of asbestos exposure in Japan. *Cancer Science*, **110**, 1076, **2019**.
62. AGOSTINO D.C. Asbestos ingestion and gastrointestinal cancer: a possible underestimated hazard. *Expert Review of Gastroenterology and Hepatology*, **11** (5), 419, **2017**.
63. BLOISE A., RICCHIUTI C., PUNTURO R., PEREIRA D. Potentially toxic elements (PTEs) associated with asbestos chrysotile, tremolite and actinolite in the Calabria region (Italy). *Chemical Geology*, **558**, 119896, **2020**.
64. DEMIRARSLAN K.O., KAYA A. Air pollution due to coal mining: literature review about particulate matter and methane emissions. *Scientific Mining Journal*, **56** (1), 23, **2017**.
65. BOZDOGAN SERT E., TURKMEN M., CETIN M. Heavy metal accumulation in rosemary leaves and stems exposed to traffic-related pollution near Adana-İskenderun Highway (Hatay, Turkey). *Environmental Monitoring and Assessment*, **191** (9), 1, **2019**.
66. CESUR A., ZEREN CETIN I., ABO AISHA A., ALRABITI O., ALJAMA A., JAWED A. A., CETIN M., SEVIK H., OZEL H. B. The usability of Cupressus arizonica annual rings in monitoring the changes in heavy metal concentration in air. *Environmental Science and Pollution Research international*, **28** (27), 35642, **2021**.
67. MOSSI M.M.M. Determination of heavy metal accumulation in the some of landscape plants for shrub forms Kastamonu University Institute of Science Department of Forest Engineering. PhD. Thesis, Kastamonu, Turkey, **2018**.
68. SEVIK H., CETIN M., OZEL H.B., PINAR B. Determining toxic metal concentration changes in landscaping plants based on some factors. *Air Quality, Atmosphere & Health*, **12** (8), 983, **2019**.
69. SEVIK H., CETIN M., OZTURK A., OZEL H. B., PINAR B. Changes in Pb, Cr and Cu concentrations in some bioindicators depending on traffic density on the basis of

- species and organs. *Applied Ecology and Environmental Research*, **17** (6), 12843, **2019**.
70. SHAHID M., DUMAT C., KHALID S., SCHRECK E., XIONG T., NIAZI N.K. Foliar heavy metal uptake, toxicity and detoxification in plants: A comparison of foliar and root metal uptake. *Journal of Hazardous Materials*, **325**, 36, **2017**.
 71. SEVIK H., CETIN M., OZEL H.B., OZEL S., ZEREN CETIN I. Changes in heavy metal accumulation in some edible landscape plants depending on traffic density. *Environmental monitoring and assessment*, **192** (2), 78, **2020**.
 72. SEVIK H., CETIN M., UCUN OZEL H., MOHAMMED MOSSI M.M., ZEREN CETIN I. Determination of Pb and Mg accumulation in some of the landscape plants in shrub forms. *Environmental Science and Pollution Research*, **27** (2), 2423, **2020**.
 73. BAYRAM M., BAKAN N.D. Environmental exposure to asbestos: from geology to mesothelioma. *Current Opinion in Pulmonary Medicine*, **20**, 301, **2014**.
 74. BRIAO G.D.V., DE ANDRADE J.R., DA SILVA M.G.C., VIEIRA M.G.A. Removal of toxic metals from water using chitosan-based magnetic adsorbents. A review, *Environmental Chemistry*, **18**, 1145, **2020**.
 75. DAS P.K., DAS B.P., DASH P. Chromite mining pollution, environmental impact, toxicity and phytoremediation: a review. *Environmental Chemistry Letters*, **19**, 1369, **2020**.
 76. DE GENNARO G., DAMBRUOSO P.R., LOIOTILE A.D., DI GILIO A., GIUNGATO P., TUTINO M., MARZOCCA A., MAZZONE A., PALMISANI J., PORCELLI F. Indoor air quality in schools. *Environmental Chemistry Letters*, **12**, 467, **2014**.
 77. HENDRICKX M. Naturally occurring asbestos in eastern Australia: a review of geological occurrence, disturbance and mesothelioma risk. *Environmental geology*, **57**, 909, **2009**.
 78. LEE R.J., STROHMEIER B.R., BRUKER K.L., VAN ORDEN D.R. Naturally occurring asbestos: a recurring public policy challenge. *Journal of Hazardous Materials*, **153**, 1, **2008**.
 79. MUKHERJEE A., AGRAWAL M. World air particulate matter: sources, distribution and health effects. *Environmental Chemistry Letters*, **15**, 283, **2017**.
 80. MUKHERJEE A., AGRAWAL M. Air pollutant levels are 12 times higher than guidelines in Varanasi, India. Sources and transfer. *Environmental Chemistry Letters*, **16**, 1009, **2018**.
 81. GUNTER M.E. Elongate mineral particles in the natural environment. *Toxicology and Applied Pharmacology*, **361**, 157, **2018**.
 82. International Ban Asbestos Secretariat, 2016. http://ibasecretariat.org/lka_alpha_asb_ban_280704.php **2016**.
 83. SPASIANO D., PIROZZI F. Treatments of asbestos containing wastes. *Journal of Environmental Management*, **204**, 82, **2017**.
 84. BERNSTEIN D.M., TOTH B., ROGERS R.A., SEPULVEDA R., KINZENDORF P., PHILLIPS J.I., ERNST H. Evaluation of the dose-response and fate in the lung and pleura of chrysotile-containing brake dust compared to chrysotile of crocidolite asbestos in a 28-day quantitative inhalation toxicology study. *Toxicology and Applied Pharmacology*, **351**, 74, **2018**.
 85. PAWELCZYK A., BOŹEK F. Health risk associated with airborne asbestos. *Environmental Monitoring and Assessment*, **187** (7), 1, **2015**.
 86. NAM S.N., JEONG S., LIM H. Thermochemical destruction of asbestos-containing roofing slate and the feasibility of using recycled waste sulfuric acid. *Journal of Hazardous Materials*, **265**, 151, **2014**.
 87. FERRANTE D., MIRABELLI D., SILVESTRI S., AZZOLINA D., GIOVANNINI A., TRIBAUDINO P., MAGNANI C. Mortality and mesothelioma incidence among chrysotile asbestos miners in Balangero, Italy: A cohort study. *American Journal of Industrial Medicine*, **63** (2), 135, **2019**.
 88. ZHENG B., ZANG L., LI W., LI H., WANG H., ZHANG M., SONG X. Quantitative analysis of asbestos in drinking water and its migration in mice using fourier-transform infrared spectroscopy and inductively coupled plasma optical emission spectrometry. *Analytica Chimica Acta*, **1058**, 29, **2019**.
 89. CETIN M. Landscape Engineering, Protecting Soil, and Runoff Storm Water. *Advances in Landscape Architecture - Chapter*. InTechOpen. **2013**.
 90. CETIN M. A Change in the Amount of CO₂ at the Center of the Examination Halls: Case Study of Turkey. *Studies on Ethno-Medicine*, **10** (2), 146, **2016**.
 91. KUMAR A., PRASAD M.N.V., TRIPTI., MAITI S.K. Asbestos: Resource Recovery and Its Waste Management: chapter in book. In environmental material and waste: resource recovery and pollution prevention: monograph, 285, **2016**.
 92. JOVANOVIĆ P. Mining in Serbia, Second Book - Volume One, Beograd, 869, **2008**.
 93. DEDIĆ Lj., MOŽINA A., RADULOVIĆ P., JOVOVIĆ M., JOKSIMOVIĆ D. Non metallic sources deposit of the Kopaonik area, Geology and Metallogeny of the Kopaonik Mt. Kopaonik. Beograd, 369, **1995**.
 94. PEOPLE AND ASBESTOS 1947-1957, Asbestos mine and separation „Korlaće” Brvenik 5, **1957**.
 95. MIKOV M.I. Asbestosis in workers employed in »Korlaće« asbestos mines and separation, *Archives of Occupational Hygiene and Toxicology*, **17** (1), 63, **1966**.
 96. LUKOVIĆ S. Contribution to the knowledge of geological and engineering geological properties of rocks in the narrower area of the Korlaća asbestos deposit, Fund of professional documents of the Institute for Geological and Geophysical Research, Belgrade, 57, **1960**.
 97. SPUŽIĆ V., SRBINOVIĆ LJ. The state of allergy in employees in the production of asbestos in the Korlaće mine and in the inhabitants of nearby villages, From the Proceedings of the SAN - Institute for Medical Research Department of Occupational Medicine - Book 2, Belgrade, 94, **1954**.
 98. VUKMIROVIĆ D. Population, comparative overview of the number of inhabitants 1948, 1953, 1961, 1971, 1981, 1991, 2002, data by settlements, Statistical Office of the Republic of Serbia, Belgrade, **2004**.
 99. RADULOVIĆ D. Korlaće through the centuries, Belgrade, 2, **2001**.
 100. DE ZORZI P., BARBIZZI S., BELLI M., CICERI G., FAJGELJ A., MOORE D., SANSONE U., PERK MVD. Terminology in soil sampling (IUPAC Recommendations 2005), *Pure and Applied Chemistry*, **77** (5), 827, **2005**.
 101. TEMPUS EU PROJECT Safety and health at work – Asbestos Characteristics and principles of exposure reduction, NOVI SAD, 20, **2013**.
 102. FEDER I.S., TISCHOFF I., THEILE A., SCHMITZ I., MERGET R., TANNAPFEL A. The asbestos fibre burden in human lungs: New insights into the chrysotile debate. *European Respiratory Journal*, **49**, 1602534, **2017**.

103. NEMERY B. Metal toxicity and the respiratory tract. *European Respiratory Journal*, **3**, 202, **1990**.
104. WEI B., YANG L., ZHU O., YU J., JIA X. Multivariate analysis of trace elements distribution in hair of pleural plaques patients and health group in a rural area from China. *Hair Therapy & Transplantation*, **4**, 2167, **2014**.
105. UCUN OZEL H., OZEL H. B., CETIN M., SEVIK H., GEMICI B. T., VAROL T. Base alteration of some heavy metal concentrations on local and seasonal in Bartın River. *Environmental monitoring and assessment*, **191** (9), 594, **2019**.
106. CETIN M., SEVIK H., COBANOGLU O. Ca, Cu, and Li in washed and unwashed specimens of needles, bark, and branches of the blue spruce (*Picea pungens*) in the city of Ankara. *Environmental Science and Pollution Research international*, **27** (17), 21816, **2020**.
107. SEVIK H., CETIN M., OZEL HB., AKARSU H., ZEREN CETIN I. Analyzing of usability of tree-rings as biomonitors for monitoring heavy metal accumulation in the atmosphere in urban area: a case study of cedar tree (*Cedrus* sp.). *Environmental Monitoring and Assessment*, **192** (1), 23, **2020**.
108. IARC Working Group on the Evaluation of Carcinogenic Risk to Humans, Arsenic, Metals, Fibres and Dusts, IARC Monographs on the Evaluation of Carcinogenic Risks to Humans Volume 100C, International Agency for Research on Cancer: Lyon, France **100** (Pt C), 11, **2012**.
109. IARC Working Group on the Evaluation of Carcinogenic Risks to Humans, Beryllium, Cadmium, Mercury, and Exposures in the Glass Manufacturing Industry. International Agency for Research on Cancer: Lyon, France, **58**, 1, **1993**.
110. BOSKABADY M., MAREFATI N., FARKHONDEH T., SHAKERI F., FARSHBAF A., BOSKABADY M.H. The effect of environmental lead exposure on human health and the contribution of inflammatory mechanisms, a review. *Environment International*, **120**, 404, **2018**.
111. LEYSSENS L., VINCK B., STRAETEN V.D.C., WUYTS F., MAES L. Cobalt toxicity in humans. A review of the potential sources and systemic health effects, *Toxicology*, **387**, 43, **2017**.
112. BLOISE A., PUNTURO R., CATALANO M., MIRIELLO D., CIRRINCIONE R. Naturally occurring asbestos (NOA) in rock and soil and relation with human activities: the monitoring example of selected sites in Calabria (southern Italy). *Italian Journal of Geosciences*, **135** (2), 268, **2016**.
113. CANNATA C.B., BLOISE A., DE ROSA R. Outdoor fibres air pollution monitoring in the Crotona area (Southern Italy). *Journal of Mediterranean Earth Sciences*, **10**, 27, **2018**.
114. GWENZI W. Occurrence, behaviour, and human exposure pathways and health risks of toxic geogenic contaminants in serpentinitic ultramafic geological environments (SUGEs): a medical geology perspective. *Science of the Total Environment*, **700**, 134622, **2019**.
115. RICCHIUTI C., BLOISE A., PUNTURO R. Occurrence of asbestos in soils: State of the Art. Episodes. *Journal of international geoscience*, **43** (3), 881, **2020**.
116. BLOISE A., BARCA D., GUALTIERI A.F., POLLASTRI S., BELLUSO E. Trace elements in hazardous mineral fibres. *Environmental Pollution*, **216**, 314, **2016**.
117. BALLIRANO P., BLOISE A., GUALTIERI A.F., LEZZERINI M., PACELLA A., PERCHIAZZI N., DOGAN M., DOGAN A.U. The crystal structure of mineral fibres. In *Mineral Fibres: Crystal Chemistry, Chemical-Physical Properties, Biological Interaction and Toxicity*; Gualtieri, A.F., Ed.; European Mineralogical Union: London, UK, **18**, 17, **2017**.
118. GWENZI W. Occurrence, behaviour, and human exposure pathways and health risks of toxic geogenic contaminants in serpentinitic ultramafic geological environments (SUGEs): A medical geology perspective. *Science of The Total Environment*, **700**, 134622, **2019**.
119. BLOISE A., RICCHIUTI C., LANZAFAME G., PUNTURO R. X-ray synchrotron microtomography: a new technique for characterizing chrysotile asbestos. *Science of the Total Environment*, **703**, 135675, **2020**.